



Published in final edited form as:

J Autoimmun. 2015 December ; 65: 38–48. doi:10.1016/j.jaut.2015.08.005.

Epidermal Injury Promotes Nephritis Flare in Lupus-Prone Mice

Kaitlyn L. Clark¹, Tamra J. Reed¹, Sonya J. Wolf², Lori Lowe^{3,4}, Jeffrey B. Hodgin³, and J. Michelle Kahlenberg^{1,*}

¹Division of Rheumatology, Department of Internal Medicine, University of Michigan, Ann Arbor, MI USA

²University of Michigan Program in Biomedical Sciences, University of Michigan, Ann Arbor, MI USA

³Department of Pathology, University of Michigan, Ann Arbor, MI USA

⁴Department Dermatology, University of Michigan, Ann Arbor, MI USA

Abstract

Systemic lupus erythematosus is clinically characterized by episodes of flare and remission. In patients, cutaneous exposure to ultraviolet light has been proposed as a flare trigger. However, induction of flare secondary to cutaneous exposure has been difficult to emulate in many murine lupus models. Here, we describe a system in which epidermal injury is able to trigger the development of a lupus nephritis flare in New Zealand Mixed (NZM) 2328 mice. 20-week old NZM2328 female mice underwent removal of the stratum corneum via duct tape, which resulted in rapid onset of proteinuria and death when compared to sham-stripped littermate control NZM2328 mice. This was coupled with a drop in serum C3 concentrations and dsDNA antibody levels and enhanced immune complex deposition in the glomeruli. Recruitment of CD11b⁺CD11c⁺F4/80^{high} macrophages and CD11b⁺CD11c⁺F4/80^{low} dendritic cells was noted prior to the onset of proteinuria in injured mice. Transcriptional changes within the kidney suggest a burst of type I IFN-mediated and inflammatory signaling which is followed by upregulation of CXCL13 following epidermal injury. Thus, we propose that tape stripping of lupus-prone NZM2328 mice is a novel model of lupus flare induction that will allow for the study of the role of cutaneous inflammation in lupus development and how crosstalk between dermal and systemic immune systems can lead to lupus flare.

Keywords

Lupus; Flare; Skin; Nephritis; Chemokines

*Address correspondence to J. Michelle Kahlenberg M.D., Ph.D., University of Michigan Division of Rheumatology, Department of Internal Medicine, A520A MSRB I, 1150 W. Medical Center Drive, Ann Arbor, Michigan 48109-5657. mkahlenb@med.umich.edu Telephone: 735-936-3257.

Publisher's Disclaimer: This is a PDF file of an unedited manuscript that has been accepted for publication. As a service to our customers we are providing this early version of the manuscript. The manuscript will undergo copyediting, typesetting, and review of the resulting proof before it is published in its final citable form. Please note that during the production process errors may be discovered which could affect the content, and all legal disclaimers that apply to the journal pertain.

1. INTRODUCTION

Systemic lupus erythematosus (SLE) is characterized by progressive organ damage often exacerbated by acute disease flares. Development of SLE is thought to be secondary to genetic and epigenetic predisposition which promotes autoreactive T and B cell survival following exposure to appropriate environmental stimuli (reviewed in¹). Autoantibodies and autoreactive cells can be present in a quiescent state of low disease activity. However, SLE patients will experience episodes of disease flare during which inflammation of various organs results in permanent damage. Knowledge of what drives the onset of flares in a previously stable patient is poorly understood. Viral infection has been linked to exacerbation of disease activity in some patients (reviewed in²). Exposure to ultraviolet (UV) light also may exacerbate cutaneous disease³ and can accelerate lupus nephritis in certain murine models⁴. The mechanisms promoting flares following these triggers remain poorly understood, yet they serve as important targets for development of preventative therapies for lupus flares.

Murine lupus models have been essential to dissect disease pathogenesis. These models demonstrate an accumulation of autoantibody production and autoreactive B and T cell populations followed by eventual onset of organ damage (reviewed in⁵). Thus, these models represent essentially a quiescent stage of the disease until organ damage ensues.

Acceleration of autoantibody production and acute glomerulonephritis via injection of IFN α -expressing adenovirus has been used as a model to study the onset of acute lupus⁶⁻⁸, and has been a useful tool for understanding the role of this cytokine in disease onset. Other mechanisms of disease flare have been more difficult to model in murine systems, however. UV induction of systemic disease works only in murine models with increased expression of toll-like receptor (TLR)^{7,4}. Importantly, TLR7 agonist stimulation of cutaneous inflammation and glomerulonephritis in wild-type mice requires cutaneous, not systemic application⁹, which suggests a role for skin inflammation to promote systemic disease. Epidermal injury through removal of the stratum corneum via tape application in lupus-prone NZB/NZW F₁ mice has been proposed as a valid model for the study of cutaneous lupus¹⁰. Thus, we chose to use this method of epidermal injury to study the effects of cutaneous inflammation on SLE flare in lupus prone NZM2328 mice.

2. MATERIALS AND METHODS

2.1 Mice

The University of Michigan committee on use and care of animals reviewed and approved all animal protocols for this study. NZM2328 mice were a kind gift of Dr. Chaim Jacob, University of Southern California, and were bred at the University of Michigan Breeding core. Mice were housed in specific-pathogen free housing at the University of Michigan. The NZM2328 strain was chosen as it is an excellent model for lupus nephritis in that it develops high titers of dsDNA antibodies, immune complex deposits in the kidney and is the closest congenic strain to the well-studied NZB/NZW (F₁) model¹¹. Further, this model does not spontaneously develop cutaneous disease, which allows us to study the effects of cutaneous inflammation without confounders. BALB/c mice were a kind gift from Dr. Mary O'Riordan at the University of Michigan.

2.2 Cutaneous Injury via Tape Stripping

20-week old female NZM2328 mice or 20-week old female BALB/c mice were given 1 mg buprenorphine via subcutaneous injection for analgesia followed by hair removal via shaving and application of Veet to a 3×4 cm area of dorsal skin. Urine and serum were collected and stored. The mice were anesthetized in a drop jar via isoflurane (Vet One, Fluriso) and the stratum corneum was removed by 25 applications and removal of 3M duct tape placed to the dorsal skin. Rash development and urinary protein were monitored twice a week. Sham animals were given buprenorphine followed by anesthetization via isoflurane, hair removal via shaving and application of Veet, but they did not undergo duct tape application. See Table 1 for summary of treatments and sample collection.

2.3 Characterization of anti-double stranded DNA and C3 serum levels

Serum anti-dsDNA and C3 levels were quantified via ELISA (Alpha Diagnostic International, San Antonio, TX and Innovative Research Inc., Novi, MI), according to manufacturer's protocols.

2.4 Proteinuria analysis

Prior to euthanasia, urine samples were collected and assessed for microalbumin using Albuwell kits (Exocell, Philadelphia, PA) and total creatinine (Cr) using a commercial kit (Bioassay Systems, Hayward, CA). Ratios of microalbumin:Cr were calculated to estimate 24 hour urinary protein excretion.

2.5 Renal Histopathology and Immune Complex Deposition Scoring

To score glomerular inflammation (activity index) and scarring (chronicity index), kidneys perfused with 10 U/ml heparin sulfate (Sigma) in PBS were fixed in 10% formalin, paraffin embedded, and section at 3 μm thickness. Periodic Acid Schiff (PAS)-stained sections were examined and graded (JBH) in a blinded manner as previously described by us and others^{12,13}. Briefly, a semiquantitative scoring system assessed 3 different parameters of activity (mesangial hypercellularity, crescents and endocapillary cellular infiltrate) in 30 glomeruli per mouse. Scores were defined as: 0=no involvement, 0.5=minimal involvement (<10%), 1=mild involvement (10–30%), 2=moderate involvement (31–60%), 3=severe (>60%). The activity index was generated by combining the scores for mesangial hypercellularity, crescents, and endocapillary cellularity for each glomerulus and calculating the average for each mouse. The chronicity index was likewise generated by combining the scores for mesangial sclerosis, capillary sclerosis, and organized crescents and calculating the average for each mouse.

Glomerular immune complex deposition was quantified on 6μm frozen kidney sections via staining for C3 and IgG deposition as previously described¹³. Briefly, sections were stained with FITC-conjugated anti-C3 (ICL, Portland, OR) and Texas-red-conjugated anti-mouse IgG (Sigma) for 1 h at 4°C; Hoechst (Invitrogen, Eugene, OR) was used to visualize DNA. Immune complex staining was quantified using Metamorph v7.0. 6 glomeruli per mouse were analyzed. Integrated FITC and Texas Red staining was calculated and presented as staining per area.

2.6. Microscopy

Photomicrographs of PAS-stained renal sections and H&E stained skin sections were captured using an Olympus BX41 microscope with 40× objective. Photos of immune complex staining were captured at the Center for Live Cell Imaging (CLCI) at the University of Michigan Medical School using an Olympus IX70 inverted microscope (Olympus; Center Valley PA) and a 40× objective.

2.7 Flow Cytometry

Following euthanasia and renal perfusion as above, one whole kidney was removed for flow cytometry analysis. Tissue was minced and then digested with 0.1mg/mL Liberase (Roche), 200 U/mL DNase (Roche) and 2.4 mM CaCl₂ in DMEM (Invitrogen) at 37°C in a humidified incubator for 1 hr. Tissue was then passed through a 70µm cell strainer; RBCs were lysed with multi-species RBC lysis buffer (eBioscience) and live cells were counted via trypan blue exclusion. Cells were stained for one hour on ice using the following antibodies (all from BioLegend, San Diego, CA): CD19-PECy7, CD3-APC, Ly6G-Fitc, F4/80-PE, B220-APC, CD138-PE, CD11b-APC, CD11c-PECy7, CD11c-PE, and Ly6C-PECy7. Flow data was collected on a BD LSR II flow cytometer and analyzed via FlowJo VX.0.7 (Tree Star).

2.8 Real-time PCR

Renal tissue was homogenized in TriPur (Roche) and RNA was purified via Direct-zol mini RNA prep (Zymo). RNA (100ng) was transcribed into cDNA and quantitative real-time PCR analysis was completed on an ABI PRISM 7900HT (Applied Biosystems). Primers were as follows (all listed 5' → 3'): *Monocyte chemoattractant protein-1 (MCP-1)* AGGTCCTGTGTCATGCTTCTG (forward), GGATCATCTTGCTGGTGAAT (reverse); *Absent in melanoma-2 (AIM2)* CCAAACCCAGACACTATTGC (forward), TGTTCCCTCCTATAGCGTTGC (reverse); *Cathelicidin antimicrobial peptide (CAMP)* TCAACCAGCAGTCCCTAGAC (forward), AAGGCACATTGCTCAGGTAG (reverse); *Myxovirus (influenza virus) resistance 1 (Mx1)* GATCCGACTTCACTTCCAGATGG (forward), CATCTCAGTGGTAGTCAACCC (reverse); *Interferon alpha (IFN α common primer)* ATGGCTAGRCTCTGTGCTTTCCT (forward), AGGGCTCTCCAGAYTTCTGCTCTG (reverse); *Interferon beta (IFN β)* AGCTCCAAGAAAGGACGAACAT (forward), ATTCTTGCTTCGGCAGTTAC (reverse); *IFN regulatory factor 7 (IRF-7)* TGCTGTTTGGAGACTGGCTAT (forward), TCCAAGCTCCCGGCTAAGT (reverse); *chemokine (C-C motif) receptor 1 (CCR1)* TGGGCAATGTCTAGTGATT (forward), GCATACCAAAAATCCAGTC (reverse); *IFN-inducible protein 10 (IP-10)* ATCATCCCTGCGAGCCTAT (forward), ATTCTTGCTTCGGCAGTTAC (reverse); *ISG15 ubiquitin-like modifier (ISG15)* CAGAAGCAGACTCCTTAATTC (forward), AGACCTCATATATGTTGCTGTG (reverse); *chemokine (C-C motif) ligand 4 (CCL4)* AGCAACACCATGAAGCTCTG (forward), CTGTCTGCCTCTTTTGGTCA (reverse); *chemokine (C-C motif) ligand 5 (CCL5)* CAATCTTGCAGTCGTGTTTG (forward), GGAGTGGGAGTAGGGGATTA (reverse); *IFN- γ* AGCGGCTGACTGAACTCAGATTGTA (forward), GTCACAGTTTTTCAGCTGTATAGGG (reverse); *C-X-C motif chemokine 13 (CXCL13)*

AGAGGTTTGGCAGATGGACT (forward), GAGCCTGGACCTTTAAGCTG (reverse); β -Actin TGGAAATCCTGTGGCATCCTGAAAC (forward), TAAAACGCAGCTCAGTAACAGTCCG (reverse); Chemokine (C-C motif) ligand 20 (CCL20) CGACTGTTGCCTCTCGTACA (forward), AGGAGGTTACAGCCCTTTT (reverse); IL-18 ACTGTACAACCGCAGTAATACGC (forward), AGTGAACATTACAGATTTATCCC (reverse); Tumor necrosis factor alpha (TNF α) CCCACTCTGACCCCTTTACT (forward), TTTGAGTCCTTGATGGTGGT (reverse); IL-1 β CCCTGCAGCTGGAGAGTGTGGA (forward), CTGAGCGACCTGTCTTGGCCG (reverse); caspase-1 GACTGGGACCCTCAAGTTTT (forward), CCAGCAGCAACTTCATTTCT (reverse); Interleukin 10 (IL-10) AGTGGAGCAGGTGAAGAGTG (forward), TTCGGAGAGAGGTACAAACG (reverse); NLRP3 ATGCTGCTTCGACATCTCCT (forward), AACCAATGCGAGATCCTGAC (reverse); IL-1 receptor antagonist (IL-1RN) GCTCATTGCTGGTACTTACAA (forward), CCAGACTTGGCACAAGACAGG (reverse); suppressor of cytokine signaling 1 (SOCS1) CTGCGGCTTCTATTGGGGAC (forward), AAAAGGCAGTCGAAGGTCTCG (reverse); tumor growth factor β (TGF β) CTCCCGTGGCTTCTAGTGC (forward), GCCTTAGTTTGGACAGGATCTG (reverse).. Samples were normalized to β -actin. Fold change ($2^{-\Delta\Delta CT}$) was calculated comparing tape stripped to sham injured specimens.

2.9 Statistical Analysis

All statistical analysis was completed with the use of GraphPad Prism 6.0. Comparison between groups was completed via two-tailed student's t-test with Welch's correction for normally distributed data and via Mann-Whitney for non-normally distributed data. Correlation analysis between serum measurements and time to onset of proteinuria was completed via linear regression. Survival analysis following tape stripping was completed via Log-rank test.

3.1. Epidermal injury results in rapid nephritis flare in lupus-prone NZM 2328 mice

At 20 weeks of age, lupus-prone NZM mice have serologic manifestations of autoimmunity such as positive ANA and anti-double-stranded DNA (dsDNA) antibodies¹⁴, but do not have evidence of active organ inflammation. Following epidermal injury via duct tape, NZM 2328 mice develop a prolonged rash which lasts up to 76 days in mice that survived for that time frame (Figure 1A). The rash is characterized by increased epidermal neutrophilic inflammation within 24 hours without the presence of inflammation in the deeper dermis. At 7 days post-injury, epidermal hyperplasia, mild dermal fibrosis and chronic inflammation are present. At euthanasia (day 69 for mouse shown), the skin demonstrates regeneration of the stratum corneum, and injured mice have developed evidence of mild dermal chronic inflammation composed of lymphocytes and fairly numerous mast cells (Figure 1B), consistent with previous reports¹⁰. During observation following skin injury, a surprising and highly significant ($p=0.014$) increase in profound proteinuria was noted in mice exposed to tape injury but not in sham-treated littermate controls with a median survival of 56 days post injury. A similar enhancement of proteinuria development was not seen in age and gender-matched BALB/c mice subjected to similar procedures (Figure 1C). PAS staining of kidney sections of injured NZM2328 mice at onset of 3+ proteinuria (via dipstick) or sham-

treated littermates revealed enlarged, hypercellular glomeruli with inflammatory cell infiltrates and protein tubular casts only in injured mice, consistent with the onset of nephritis (Figure 1D). Similar changes were not seen in injured BALB/c mice (Figure 1D). Proteinuria was confirmed via albumin/Cr ratios and was found to rise starting 15 days after skin injury and increased significantly by 5 weeks post injury ($p=0.01$) (Figure 1D). No acceleration of proteinuria or nephritis was seen in 10 week old mice subjected to similar tape stripping (data not shown). Evaluation of lung, liver and cardiac pathology did not reveal evidence of organ damage or inflammation following skin injury. Further, there was no difference in white blood cell count, platelet count or hemoglobin between sham or injured animals (data not shown). These results suggest that the acceleration of nephritis was the main lupus-related phenotype following skin injury.

Many patients with SLE have elevated levels of antibodies directed against double-stranded DNA (dsDNA). NZM2328 mice also develop these antibodies and lowering of anti-dsDNA titers may correlate with tissue deposition and nephritis onset¹⁴. We thus quantified dsDNA antibody titers in our mice. As shown in Figure 2A, there was a significantly ($p=0.007$) lower titer of dsDNA antibodies in injured vs. sham treated NZM2328 mice 30 days after injury. Importantly, this drop in dsDNA antibody titers significantly correlated ($p=0.047$) with the early onset of proteinuria in injured mice (Figure 2B). Surprisingly, BALB/c mice, which had minimal levels of dsDNA antibodies at baseline, developed a significant increase ($p=0.047$) in dsDNA antibody titers 130 days after skin injury (Figure 2C), although levels were much less than those seen in NZM2328 mice. Complement C3 levels are also a marker of disease activity in SLE patients, as C3 will drop during acute flares and often heralds the presence of active nephritis. We measured C3 levels in our mice and noted a similar pattern to dsDNA levels, in that C3 levels dropped after skin injury and this trended ($p=0.07$) to correlate with the rapidity of proteinuria onset (Figures 2 D and E). No drop in C3 levels was noted in BALB/c mice (Figure 2F). Circulating DNA was also measured following skin injury, and while early detection of changes in DNA levels was not noted in pooled analysis of mice (Figure 2G), there was a highly significant ($p=0.019$) correlation between the drop in detectable serum DNA by day 14 and the rate in which proteinuria developed following skin injury (Figure 2H). These data suggest that immune complex formation, as characterized by drops in dsDNA antibody titers, serum C3 and serum DNA concentrations are a consequence of skin injury in NZM2328 mice.

3.2. Immune complex deposition is enhanced following cutaneous injury

In situ formation and entrapment of passively circulating immune complexes are proposed to contribute to the development of lupus nephritis (reviewed in¹⁵). Additionally, the drop in dsDNA antibodies, C3 levels and circulating serum DNA were all suggestive of immune complex formation in injured mice. Thus, we examined the deposition of immune complexes within the kidney following epidermal injury. As shown in Figure 3, mice exposed to skin injury had significant (IgG $p=0.06$, C3 $p=0.02$) increases in immune complex deposition in their kidneys by day 15 following skin injury. These results suggest that enhanced renal immune complex deposition is an early event following skin injury.

3.3. Epidermal Injury promotes dendritic cell and macrophage recruitment

As we detected the rapid onset of proteinuria and glomerular inflammation (Figure 1) subsequent to skin injury, we wanted to determine how skin injury influenced the early, pre-proteinuric, stages of renal inflammation. Mice that developed proteinuria before day 15 were excluded from analysis in order to assess pre-nephritic changes. As shown in figure 4A and 4C, renal activity scores trended towards increased inflammation but did not reach statistical significance ($p=0.06$) by day 15. Chronicity indices, a reflection of the duration of renal inflammation (as noted via scarring), were not affected (Figure 4B). These results suggest that while cutaneous injury results in a detectable accelerated deposition of immune complexes following skin injury, the detection of histologic inflammatory changes follows immune complex deposition.

The development of lupus nephritis has been characterized by inflammatory infiltrates of T cell ($CD8^+CD4^-$), B cell, $F4/80^{hi}$ macrophage populations, and $CD11c^+CD11b^+,F4/80^{low}$ dendritic cells (DC)¹⁶⁻¹⁸. To better characterize the inflammatory changes occurring within the kidney after skin injury, prior to proteinuria onset, we examined the inflammatory cell populations in the kidneys of pre-proteinuric mice 7 and 15 days following initial skin injury to see whether skin injury promoted early recruitment of pathogenic cell populations. Gating strategies are shown in Figure S1A and B. As shown in Figure 5A, no significant changes in neutrophil populations were noted 7 or 15 days following skin injury in mice without proteinuria. This is consistent with known data in nephritic mice¹⁸. Global assessment of macrophage populations via F4/80 staining were also unchanged. T cells remained unchanged and there was a non-significant trend for increased $CD19^+$ cells at day 15 following skin injury (Figure 5A). Early recruitment of renal $CD11b^+CD11c^+F4/80^{low}$ DCs and $CD11b^+CD11c^+F4/80^{high}$ macrophages have been described as essential for nephritis development and have been demonstrated in nephritic kidneys of several murine models of lupus^{18,19}. By day 7 following skin injury, we detected a significant ($p=0.02$) increase in $CD11b^+CD11c^+F4/80^{hi}$ macrophages in the kidneys of injured mice which persisted at day 15. Detailed characterization of the macrophage and DC populations revealed no difference in plasmacytoid dendritic cell ($B220^+CD19^-CD138^+$) populations. However, total DC ($Ly6C^+Ly6G^-CD11c^+$) populations and $CD11b^+CD11c^+F4/80^{low}$ DCs were significantly increased by 15 days post skin injury ($p=0.02$ and $p=0.03$ respectively) (Figure 5B). Similar results were noted when absolute numbers of cells per kidney were calculated (data not shown). This suggests that recruitment of $CD11b^+CD11c^+F4/80^{hi}$ macrophages followed by $CD11b^+CD11c^+F4/80^{low}$ DCs are the first detectable significant cellular change prior to nephritis development.

In a separate analysis, mice that had developed proteinuria by day 15 following skin injury had inflammatory cell profiles consistent with known nephritic changes^{16,18,19} including elevations in $CD11b^+CD11c^+F4/80^{hi}$ macrophages, T cell and B cell populations (Figure S1C). These results suggest that nephritis accelerated by epidermal injury is similar to nephritis that develops as part of natural disease progression as reported by others^{16,18,19}.

3.4. Renal interferon and inflammatory responses are increased within the kidney by day 7 post cutaneous injury and are followed by upregulation of CXCL13

As Immune complexes can promote TLR signaling within the kidney^{20–22}, we chose to examine changes in expression of various inflammatory and chemotactic factors within the kidney 7 and 15 days following skin injury. As shown in Figure 6A and B, by day 7 following skin injury, elevation of type I IFNs and type I IFN response genes are seen and this IFN response resolves (except for IRF7 upregulation) by day 15. At day 7, a striking increase in TNF α is also noted which also resolves by day 15. Pro-inflammatory genes, including upregulation of NLRP3, an inflammasome scaffold with a role in lupus nephritis^{13,23,24}, is also noted following cutaneous injury and this upregulation persists through day 15. Anti-inflammatory genes, with the exception of IL-10 are not upregulated at day 7 or day 15 following skin injury. Importantly, by day 15, a significant increase in CXCL13 is noted (Figure 6B). This chemokine has been identified as an early marker in both murine and human lupus nephritis²⁵. These results suggest that cutaneous injury results in defined signaling changes within the kidney that promote type I IFN responses, inflammasome activation and upregulation of CXCL13.

4. Discussion

Here we describe a novel model of lupus flare induced by tape stripping. This epidermal injury results in removal of the stratum corneum and acute neutrophilic inflammation within the epidermis. This is followed by accelerated immune complex deposition in the kidney, recruitment of CD11b⁺CD11c⁺F4/80^{high} and CD11b⁺CD11c⁺F4/80^{low} DCs prior to nephritis onset, and generation of defined expression changes within the kidney which promote recruitment of and reflect known pathophysiologic changes associated with lupus nephritis. Our model does not work in pre-autoimmune NZM2328 mice, suggesting that pre-formed DNA antibodies are required for nephritis induction, thus proposing skin injury as a stressor which is able to induce the development of a nephritis flare in an otherwise “stable” lupus mouse. The timing of nephritis development in our model is similar to that reported with IFN α -driven lupus exacerbation^{6,8} where development of nephritis is seen within 14–42 days. Similarly, we see enhancement of early type I IFN responses and immune complex deposition within the glomeruli following cutaneous injury. However, our model has several distinctions. First, it requires pre-existing autoimmunity in that tape stripping does not accelerate disease in 10-week old mice whereas IFN α administration does^{6,8}. Thus, our model is more reflective of the effects of cutaneous inflammation on stable lupus, and thus serves as a representation of flare. Secondly, we do not see a promotion of autoimmunity after tape stripping in NZM2328 mice as our mice show a drop in dsDNA titers, which correlates with accelerated proteinuria, rather than a rise in autoantibody production which has been reported with IFN α administration⁷. This is consistent with previous reports that suggest declines in anti-dsDNA titer and serum DNA levels correlate with immune complex deposition in the tissues and disease flare^{26,27}. Epidermal injury of BALB/c mice also did not result in nephritis; intriguingly, however, it did result in an increased rise in dsDNA antibody titers in injured but not sham treated mice. This suggests there may be a role for skin injury in promoting autoimmunity in wild-type mice. This would be consistent with

other work which has shown that epidermal overexpression of inflammatory cytokines like IFN γ can drive autoimmunity development²⁸. This finding warrants further investigation.

Following epidermal injury, we are able to detect defined transcriptional changes within the kidney which support the role of immune complex mediated signaling as an initiator of renal injury. Immune complexes containing nucleosomes and anti-dsDNA antibodies have been shown to be an initiating factor for lupus nephritis²¹. Pathogenic mechanisms include stimulation of chemokine production from mesangial cells within the kidney^{21,29} as well as immune complex stimulation of dendritic and plasmacytoid dendritic cell toll-like receptors and renal macrophages^{22,30-32}. Importantly, immune complex-mediated injury has been shown to induce recruitment of CD11c⁺ cells to the glomeruli within 7 days of deposition²⁶, and our data supports this model.

Following injury, our mice develop defined transcriptional changes within the kidney. We detect a rise in type I IFN response genes within the kidney and the upregulation of IRF7 remains persistent in the pre-nephritis state. Additionally, early production of TNF α within the kidney following skin injury is consistent with reports of TNF α elevations in active lupus³³. TNF α can also facilitate CD11c⁺ dendritic cell recruitment to the tubulointerstitial compartment of the kidney²⁶ in a non-TNFR2 dependent manner²⁷. In addition to TNF α , other NF κ B dependent genes, such as NLRP3 are upregulated following tape stripping. The NLRP3 inflammasome is an important contributor to lupus nephritis^{13,23,24}, and the contributions of this complex in renal inflammation should be further explored. We did not detect changes in anti-inflammatory gene expression, with the exception of IL-10, following skin injury. This may reflect the unusual behavior of IL-10 in lupus in that this gene has abnormal regulation in the presence of type I IFN³⁴ and has been shown to be elevated in active lupus nephritis³⁵.

Importantly, we also see evidence of defined chemokine changes within the kidney after tape stripping. Renal CCL4 transcripts are significantly increased within 7 days of tape stripping. This chemokine serves as a monocyte attractant and has been reported to attract T cells as well³⁶. CCL4/MIP-1 β has been described as elevated in murine lupus in the LPR model after the onset of nephritis has occurred³⁷. CCL4 is upregulated downstream of TLR signaling³⁶ and has been shown to promote type I IFN responses after immune complex stimulation of plasmacytoid dendritic cells³⁸. Our data suggest that CCL4 may also be activated, at least transiently, within the glomeruli before nephritis onset and may thus contribute to the recruitment of CD11b⁺CD11c⁺F4/80^{low} DCs. Further, we detect a rise in CXCL13 by day 15. CXCL13 has recently received attention for its role as a very early marker for nephritis onset²⁵.

It is able to upregulate CXCR5 in podocytes and also upregulates the expression of the chemokines CXCL1, CXCL12, macrophage migration inhibitory factor and leukemia inhibitory factor as well as podocyte migratory factors¹¹. The primary source of CXCL13 in nephritis is CD11b⁺CD11c⁺ dendritic cells and DC11b⁺CD11c^{int} macrophages^{17,39}, and our data suggest that the rise of CXCL13 in the kidney occurs concurrently with a rise in these cell populations. The role of CCL4 and CXCL13 in nephritis initiation will be important considerations for future studies.

In summary, we have described a novel model of lupus flare induction mediated by epidermal injury in lupus-prone NZM2328 mice. This model results in dermal and epidermal inflammation, immune complex deposition in the kidney, recruitment of CD11b⁺CD11c⁺F4/80^{low} DCs and CD11b⁺CD11c⁺F4/80^{high} macrophages and CXCL13 production followed by florid nephritis. Further research utilizing this model will help to determine the role of defined signaling pathways in dermal inflammation and renal disease.

Supplementary Material

Refer to Web version on PubMed Central for supplementary material.

ACKNOWLEDGEMENTS

This work was supported by the Arthritis National Research Foundation (to JMK), University of Michigan's George M. O'Brien Kidney Translational Research Core Center, 2P30-DK-081943, funded by NIH/NIDDK (to JMK) and by the National Institute of Arthritis and Musculoskeletal and Skin Diseases of the National Institutes of Health under Award Number K08AR063668 (to JMK). JBH received support through the NIH via PHS grant K08DK088944. SJW was supported by the research training in experimental immunology training grant under Award Number T32AI007413.

Abbreviations

AIM2	absent in melanoma 2
CAMP	cathelicidin antimicrobial peptide
CCL	chemokine (c-c) ligand
CCR	chemokine (c-c) receptor
cxcl	chemokine (c-x-c) ligand
IFN	interferon
IRF	interferon regulatory factor
MCP	monocyte chemoattractant protein
MX	myxovirus resistance
NZM	New Zealand Mixed
SLE	systemic lupus erythematosus
TLR	toll-like receptor
TNF	tumor necrosis factor
UV	ultraviolet

REFERENCES

1. Marion T, Postlethwaite A. Chance, genetics, and the heterogeneity of disease and pathogenesis in systemic lupus erythematosus. *Semin Immunopathol.* 2014;1–23. [PubMed: 25487033]
2. Nelson P, Rylance P, Roden D, Trela M, Tugnet N. Viruses as potential pathogenic agents in systemic lupus erythematosus. *Lupus.* 2014; 23:596–605. [PubMed: 24763543]

3. Sanders CJ, et al. Photosensitivity in patients with lupus erythematosus: a clinical and photobiological study of 100 patients using a prolonged phototest protocol. *Br J Dermatol.* 2003; 149:131–137. doi:5379 [pii]. [PubMed: 12890206]
4. Ansel JC, Mountz J, Steinberg AD, DeFabo E, Green I. Effects of UV Radiation on Autoimmune Strains of Mice: Increased Mortality and Accelerated Autoimmunity in BXSB Male Mice. *J Investig Dermatol.* 1985; 85:181–186. [PubMed: 3897390]
5. Perry D, Sang A, Yin Y, Zheng YY, Morel L. Murine models of systemic lupus erythematosus. *Journal of biomedicine & biotechnology.* 2011; 2011:271694. [PubMed: 21403825]
6. Dai C, et al. Interferon alpha on NZM2328.Lc1R27: Enhancing autoimmunity and immune complex-mediated glomerulonephritis without end stage renal failure. *Clinical Immunology.* 2014; 154:66–71. doi:<http://dx.doi.org/10.1016/j.clim.2014.06.008>. [PubMed: 24981059]
7. Liu Z, et al. Interferon-alpha accelerates murine systemic lupus erythematosus in a T cell-dependent manner. *Arthritis Rheum.* 2011; 63:219–229. [PubMed: 20954185]
8. Jacob N, et al. B Cell and BAFF Dependence of IFN- α –Exaggerated Disease in Systemic Lupus Erythematosus-Prone NZM 2328 Mice. *The Journal of Immunology.* 2011; 186:4984–4993. [PubMed: 21383240]
9. Yokogawa M, et al. Epicutaneous Application of Toll-like Receptor 7 Agonists Leads to Systemic Autoimmunity in Wild-Type Mice: A New Model of Systemic Lupus Erythematosus. *Arthritis Rheumatol.* 2014; 66:694–706. [PubMed: 24574230]
10. Guiducci C, et al. Autoimmune skin inflammation is dependent on plasmacytoid dendritic cell activation by nucleic acids via TLR7 and TLR9. *J Exp Med.* 2010; 207:2931–2942. doi:jem.20101048 [pii] 10.1084/jem.20101048. [PubMed: 21115693]
11. Jacob CO, et al. Pivotal Role of Stat4 and Stat6 in the Pathogenesis of the Lupus-Like Disease in the New Zealand Mixed 2328 Mice. *The Journal of Immunology.* 2003; 171:1564–1571. [PubMed: 12874250]
12. Zhao W, et al. The peroxisome proliferator-activated receptor gamma agonist pioglitazone improves cardiometabolic risk and renal inflammation in murine lupus. *J Immunol.* 2009; 183:2729–2740. doi:jimmunol.0804341 [pii] 10.4049/jimmunol.0804341. [PubMed: 19620300]
13. Kahlenberg JM, et al. An essential role of caspase 1 in the induction of murine lupus and its associated vascular damage. *Arthritis Rheumatol.* 2014; 66:152–162. [PubMed: 24449582]
14. Waters ST, et al. Breaking tolerance to double stranded DNA, nucleosome, and other nuclear antigens is not required for the pathogenesis of lupus glomerulonephritis. *J Exp Med.* 2004; 199:255–264. [PubMed: 14718514]
15. Lech M, Anders H-J. The Pathogenesis of Lupus Nephritis. *Journal of the American Society of Nephrology.* 2013
16. Lourenço EV, Wong M, Hahn BH, Palma-Diaz MF, Skaggs BJ. Laquinimod Delays and Suppresses Nephritis in Lupus-Prone Mice and Affects Both Myeloid and Lymphoid Immune Cells. *Arthritis & Rheumatology.* 2014; 66:674–685. [PubMed: 24574228]
17. Schiffer L, et al. Activated renal macrophages are markers of disease onset and disease remission in lupus nephritis. *J Immunol.* 2008; 180:1938–1947. [PubMed: 18209092]
18. Sahu R, Bethunaickan R, Singh S, Davidson A. Structure and Function of Renal Macrophages and Dendritic Cells From Lupus-Prone Mice. *Arthritis & Rheumatology.* 2014; 66:1596–1607. [PubMed: 24866269]
19. Triantafyllopoulou A, et al. Proliferative lesions and metalloproteinase activity in murine lupus nephritis mediated by type I interferons and macrophages. *Proc Natl Acad Sci U S A.* 2010; 107:3012–3017. [PubMed: 20133703]
20. Lövgren T, et al. Induction of interferon- α by immune complexes or liposomes containing systemic lupus erythematosus autoantigen– and Sjögren's syndrome autoantigen–associated RNA. *Arthritis & Rheumatism.* 2006; 54:1917–1927. [PubMed: 16729300]
21. Tofteland ND, Shaver TS. Clinical efficacy of etanercept for treatment of PAPA syndrome. *Journal of clinical rheumatology : practical reports on rheumatic & musculoskeletal diseases.* 2010; 16:244–245. [PubMed: 20661073]
22. Marshak-Rothstein A. Toll-like receptors in systemic autoimmune disease. *Nat Rev Immunol.* 2006; 6:823–835. [PubMed: 17063184]

23. Zhao J, et al. P2X7 blockade attenuates lupus nephritis by inhibiting NLRP3/ASC/caspase-1 activation. *Arthritis & Rheumatism*. 2013 n/a-n/a.
24. Zhao J, et al. Bay11-7082 attenuates murine lupus nephritis via inhibiting NLRP3 inflammasome and NF- κ B activation. *International Immunopharmacology*. 2013; 17:116–122. doi:<http://dx.doi.org/10.1016/j.intimp.2013.05.027>. [PubMed: 23770281]
25. Jacob CO, et al. Development of systemic lupus erythematosus in NZM 2328 mice in the absence of any single BAFF receptor. *Arthritis Rheum*. 2013; 65:1043–1054. [PubMed: 23334904]
26. Knight JS, et al. Peptidylarginine deiminase inhibition disrupts NET formation and protects against kidney, skin and vascular disease in lupus-prone MRL/lpr mice. *Annals of the Rheumatic Diseases*. 2014
27. Ho A, Magder LS, Barr SG, Petri M. Decreases in anti-double-stranded DNA levels are associated with concurrent flares in patients with systemic lupus erythematosus. *Arthritis Rheum*. 2001; 44:2342–2349. [PubMed: 11665975]
28. Seery JP, Carroll JM, Cattell V, Watt FM. Antinuclear autoantibodies and lupus nephritis in transgenic mice expressing interferon gamma in the epidermis. *J Exp Med*. 1997; 186:1451–1459. [PubMed: 9348302]
29. Menke J, et al. Sunlight triggers cutaneous lupus through a CSF-1-dependent mechanism in MRL-Fas(lpr) mice. *J Immunol*. 2008; 181:7367–7379. [PubMed: 18981160]
30. Shin MS, et al. U1-Small Nuclear Ribonucleoprotein Activates the NLRP3 Inflammasome in Human Monocytes. *The journal of immunology*. 2012; 188:4769–4775. [PubMed: 22490866]
31. Shin MS, et al. Self Double-Stranded (ds)DNA Induces IL-1 β Production from Human Monocytes by Activating NLRP3 Inflammasome in the Presence of Anti-dsDNA Antibodies. *The journal of immunology*. 2013
32. Tian J, et al. Toll-like receptor 9-dependent activation by DNA-containing immune complexes is mediated by HMGB1 and RAGE. *Nat Immunol*. 2007; 8:487–496. doi:http://www.nature.com/nature/journal/v8/n5/supinfo/ni1457_S1.html. [PubMed: 17417641]
33. Cigni A, et al. Interleukin 1, Interleukin 6, Interleukin 10, and Tumor Necrosis Factor α in Active and Quiescent Systemic Lupus Erythematosus. *Journal of Investigative Medicine*. 2014; 62:825–829. doi:10.231/JIM.0000000000000085. [PubMed: 24987977]
34. Cates AM, et al. Interleukin 10 hampers endothelial cell differentiation and enhances the effects of interferon alpha on lupus endothelial cell progenitors. *Rheumatology (Oxford, England)*. 2015; 54:1114–1123.
35. Koenig KF, et al. Serum cytokine profile in patients with active lupus nephritis. *Cytokine*. 2012; 60:410–416. doi:<http://dx.doi.org/10.1016/j.cyto.2012.07.004>. [PubMed: 22846145]
36. Bystry RS, Aluvihare V, Welch KA, Kallikourdis M, Betz AG. B cells and professional APCs recruit regulatory T cells via CCL4. *Nat Immunol*. 2001; 2:1126–1132. [PubMed: 11702067]
37. Martinon F, Burns K, Tschopp J. The inflammasome: a molecular platform triggering activation of inflammatory caspases and processing of proIL- β . *Molecular cell*. 2002; 10:417–426. [PubMed: 12191486]
38. Mariathasan S, et al. Differential activation of the inflammasome by caspase-1 adaptors ASC and Ipaf. *Nature*. 2004; 430:213–218. [PubMed: 15190255]
39. Ishikawa S, et al. Aberrant High Expression of B Lymphocyte Chemokine (Blc/Cxcl13) by C11b⁺Cd11c⁺ Dendritic Cells in Murine Lupus and Preferential Chemotaxis of B1 Cells towards Blc. *The Journal of Experimental Medicine*. 2001; 193:1393–1402. [PubMed: 11413194]

Highlights

- Lupus prone NZM2328 mice subjected to tape-stripping develop accelerated nephritis
- Immune complex deposition within the glomeruli is enhanced following epidermal injury
- Prior to proteinuria onset, CD11b⁺CD11c⁺f4/80^{high} macrophages and CD11b⁺CD11c⁺f4/80^{low} DC are recruited into the kidney
- CXCL13 expression is increased in the kidney following epidermal injury prior to the onset of proteinuria

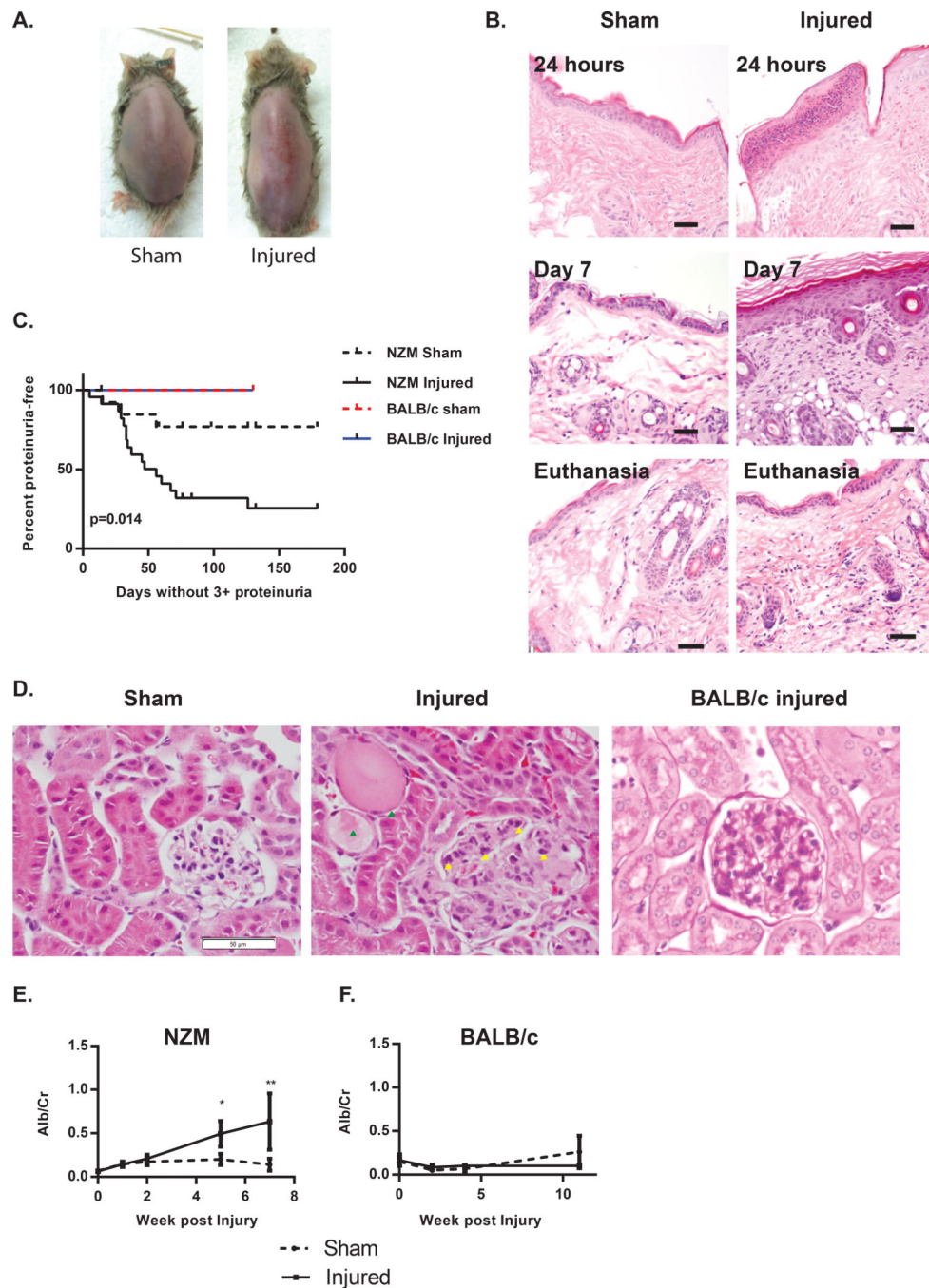


Figure 1. Epidermal injury results in rapid nephritis flare in lupus-prone NZM 2328 mice

A. Representative photograph of day 76 post injury showing healthy skin in a sham treated mouse (left) and prolonged rash in a tape-stripped mouse (right). B. Hematoxylin and eosin (H&E) stained sections of representative biopsies of back skin of sham and tape injured mice 24 hours after injury (top), 7 days post injury (middle) and at onset of proteinuria (bottom). Size bar=20 μ m. C. Graph represents survival analysis of 20-week old NZM mice exposed to cutaneous injury (n=23) or sham injury (n=14). Curve comparison via Log-rank test demonstrates a significant difference between curves, p=0.014. D. Representative PAS-

stained kidneys demonstrating characteristics of nephritis in a proteinuric mouse following skin injury. Injured mice demonstrate enlarged, hypercellular glomeruli with inflammatory infiltrate (yellow arrowheads) and tubular protein casts (green arrowheads). Control BALB/c mouse 120 days post injury is shown for comparison. Size bar=50 μ m. E. Graph represents proteinuria of NZM2328 mice as serially measured by albumin/Cr ratio in skin injured (n=29) vs. sham treated (n=20) littermates following skin injury. F. Graph represents proteinuria as serially measured by albumin/Cr ratio in BALB/c mice following skin injury (n=6) or sham treatment (n=6). *=p<0.05, **=p<0.01.

Author Manuscript

Author Manuscript

Author Manuscript

Author Manuscript

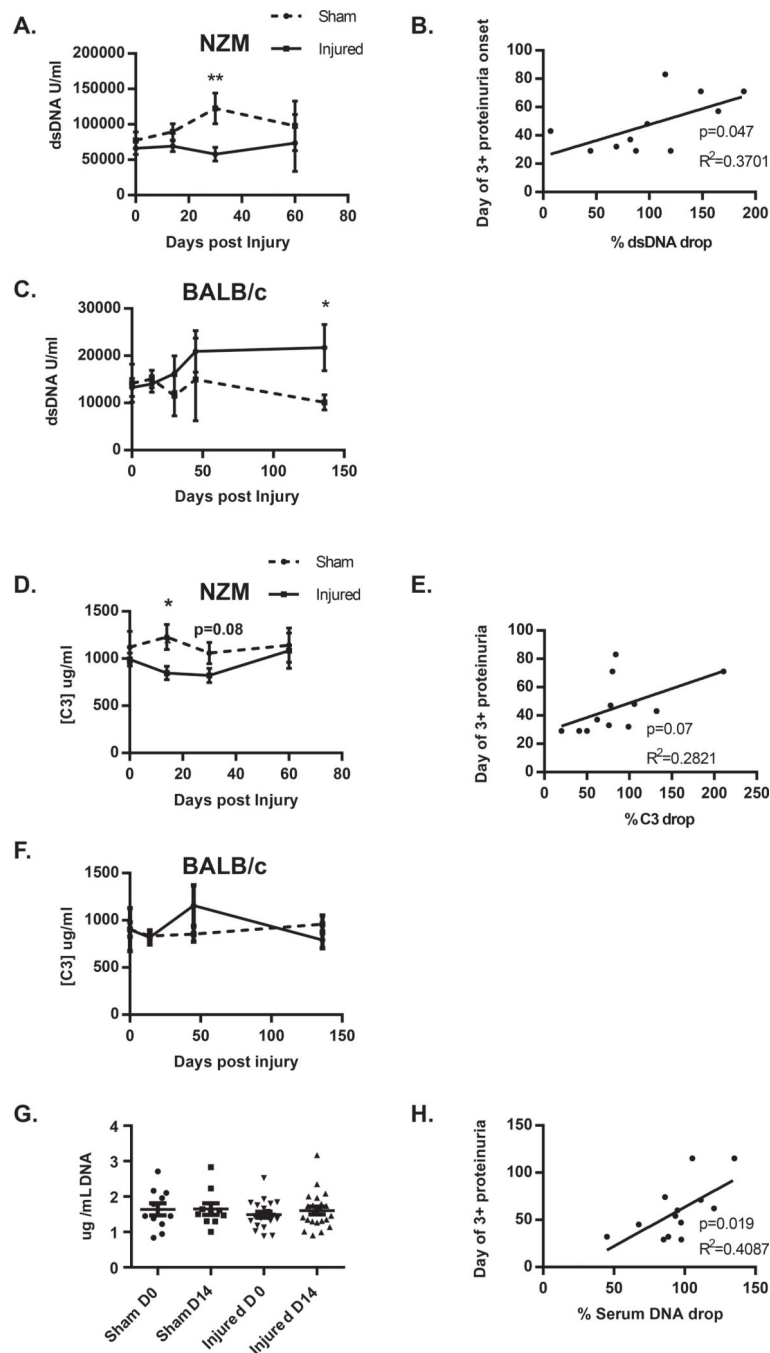


Figure 2. Epidermal injury results in a drop in dsDNA titers, C3 concentration and serum DNA, which correlates with rapid induction in proteinuria

Serum double stranded DNA titers were serially measured following skin injury in NZM (A) (n=17 for sham and n=27 for injured) and BALB/c (C) (n=6 sham and n=6 injured) mice. B. The percent by which the titer changed at day 30 was plotted versus the day of elevated proteinuria onset in skin injured mice and analyzed via linear regression. D. Serum C3 concentrations were serially measured following skin injury in NZM (D) (n=11 for sham and n=16 for injured) and BALB/c (F) (n=6 sham and n=6 injured) mice. E. The percent by which [C3] changed at day 30 was plotted versus the day of elevated proteinuria onset in

skin injured mice and analyzed via linear regression. G. Serum DNA levels were measured prior to skin injury and at day 14 post injury. H. The percent change in serum DNA from day 0 to day 14 was plotted vs. the day of proteinuria onset and analyzed via linear regression. $*=p<0.05$, $**=p<0.01$.

Author Manuscript

Author Manuscript

Author Manuscript

Author Manuscript

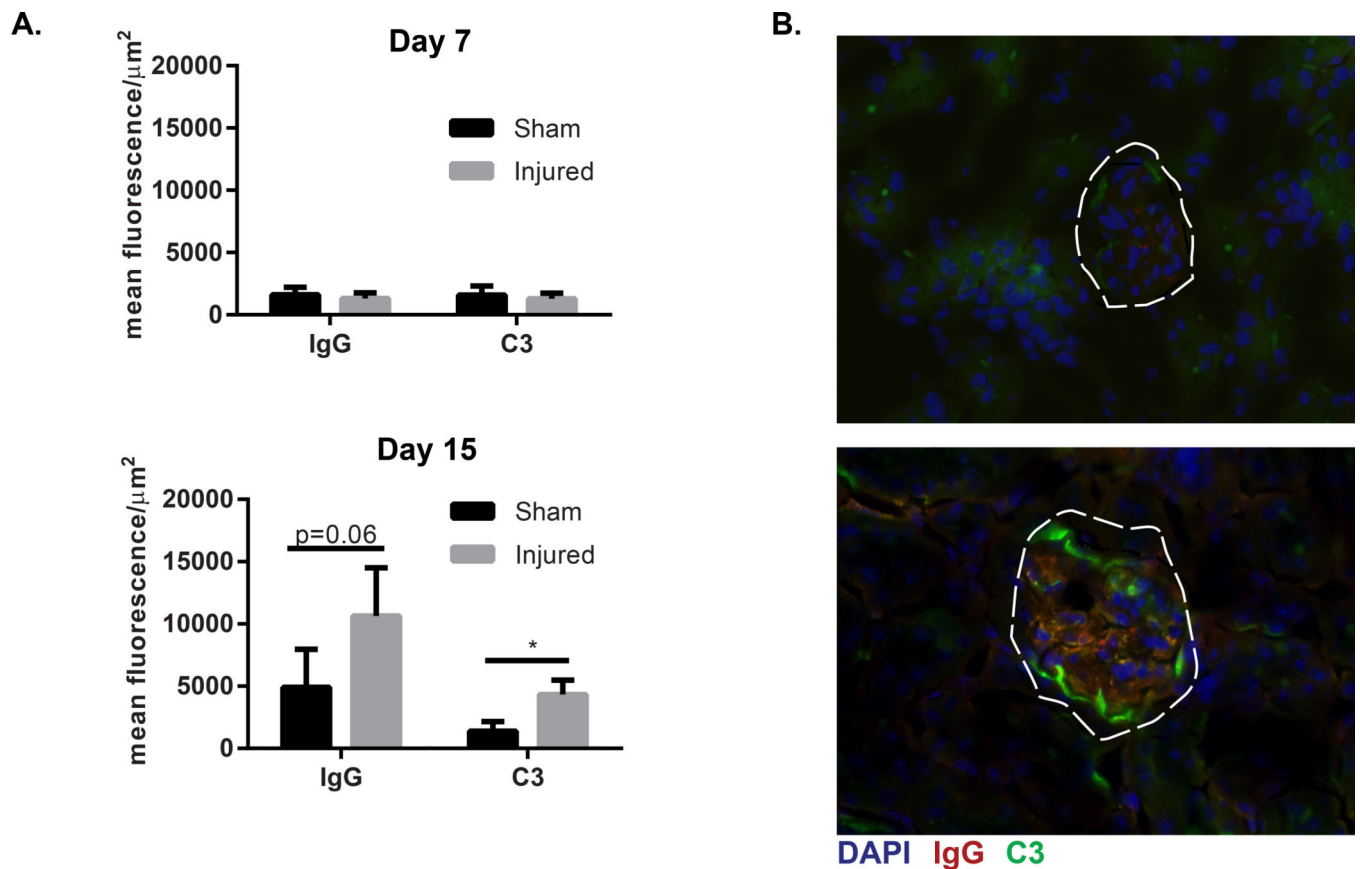


Figure 3. Immune complex deposition is enhanced following cutaneous injury

A. Quantification of immune complex staining was completed via calculation of mean fluorescence/area of 6 glomeruli per mouse in skin injured and sham-injured littermate mice euthanized day 7 and day 15 post tape stripping. For Day 7, sham treated n=6, injured n=7. For day 15, sham treated n=11, skin injured n=13. B. Representative image of immunofluorescent microscopy of renal cortex, glomeruli are outlined by white dashed line. Green=FITC-C3, Red=Texas Red-IgG, Blue=DAPI. *=p<0.05 via two-tailed unpaired students' t-test with Welch's correction..

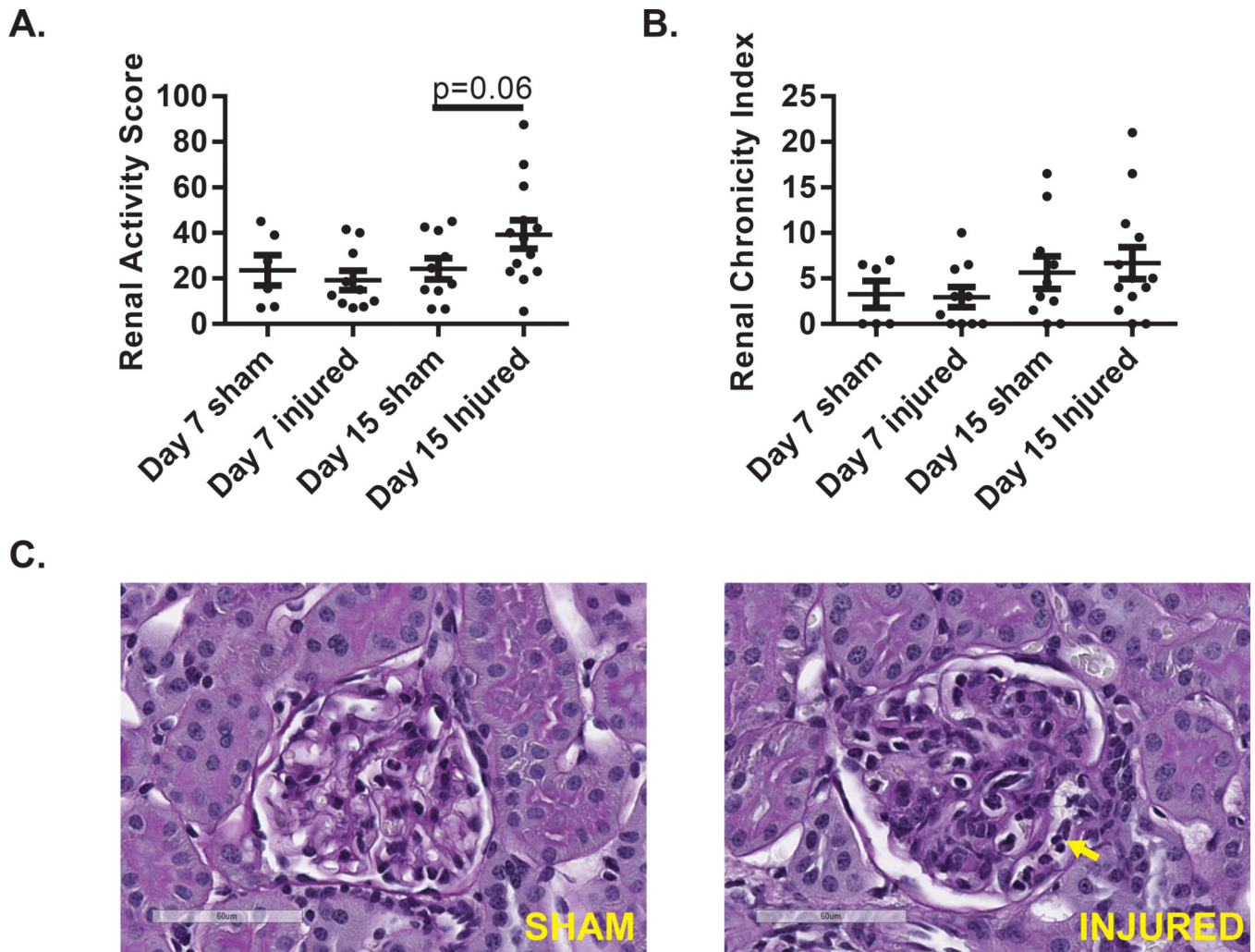
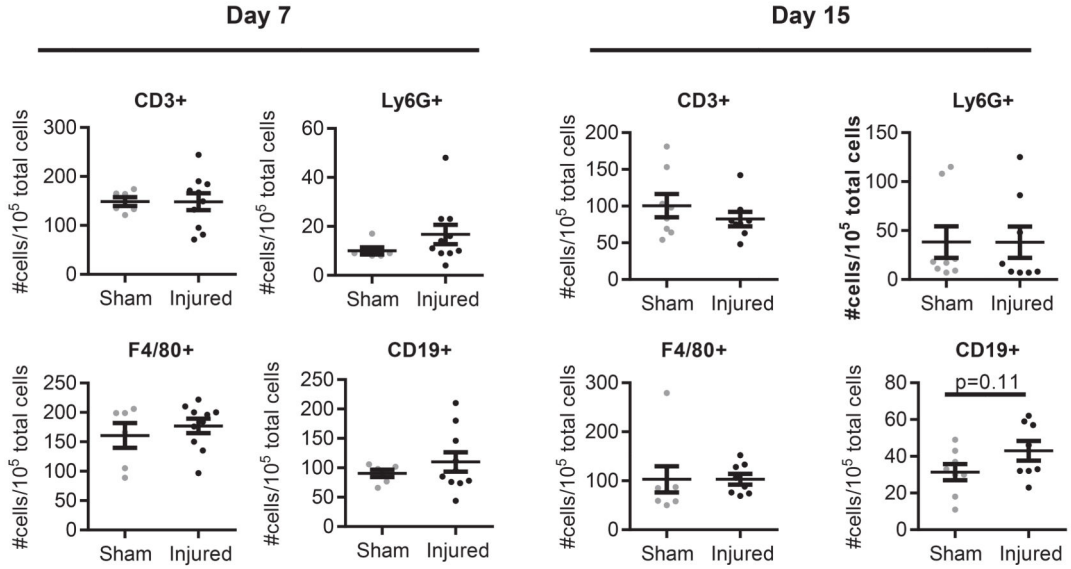


Figure 4. Renal inflammation is mild prior to onset of proteinuria

Mice undergoing tape injury or sham treated mice were euthanized 7 or 15 days following initial tape injury. Mice that developed proteinuria prior to euthanasia were excluded from analysis. Scores for A. renal activity (based on mesangial and glomerular cellularity and crescent formation) and B. chronicity (based on sclerosis) were made at 7 and 15 days following cutaneous injury. C. Representative photomicrographs of glomeruli at day 15 demonstrating (sham) normocellular glomerulus with patent capillary lumina and (injured) diffuse mesangial hypercellularity and collections of mononuclear leukocytes within capillary lumina (yellow arrow).

A.



B.

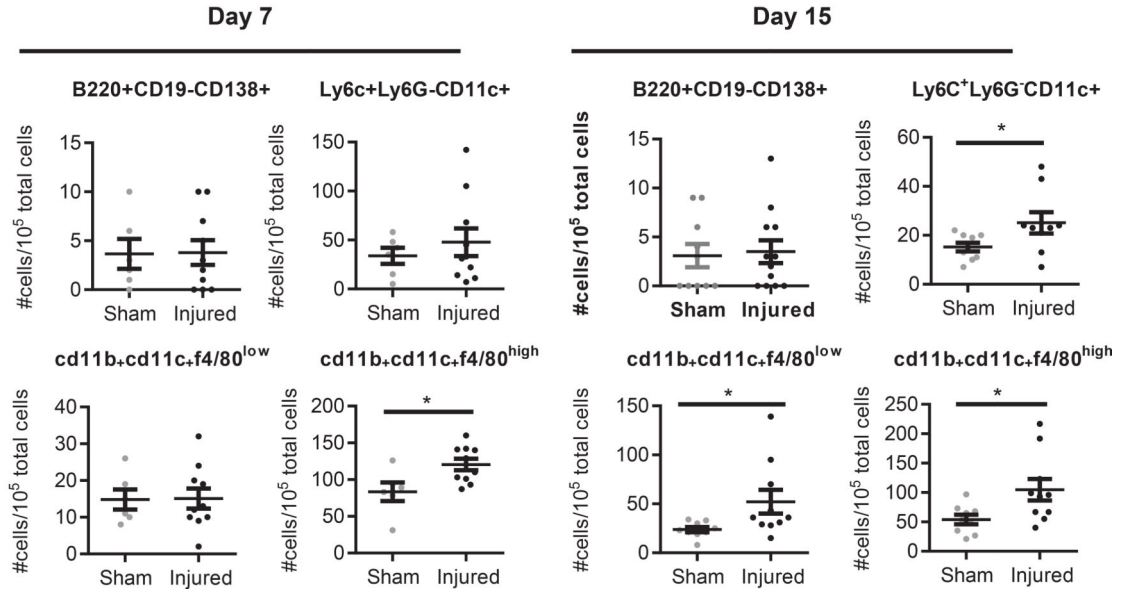


Figure 5. Tape stripping leads to recruitment of CD11b⁺CD11c⁺F4/80^{high} macrophages and CD11b⁺CD11c⁺F4/80^{low} dendritic cells prior to proteinuria onset

A. Inflammatory cell populations and B. DC and macrophage sub-populations in the kidney were evaluated by flow cytometry. Graphs represent the number positive/ 10^5 total live cellular events for each indicated marker. Data for each individual mouse examined are shown with mean \pm SEM added. For Day 7, sham treated n=6, injured n=10. For day 15, sham treated n=9, skin injured n=10. Statistical analysis was via unpaired two-sided student's t-test. *= $p < 0.05$.

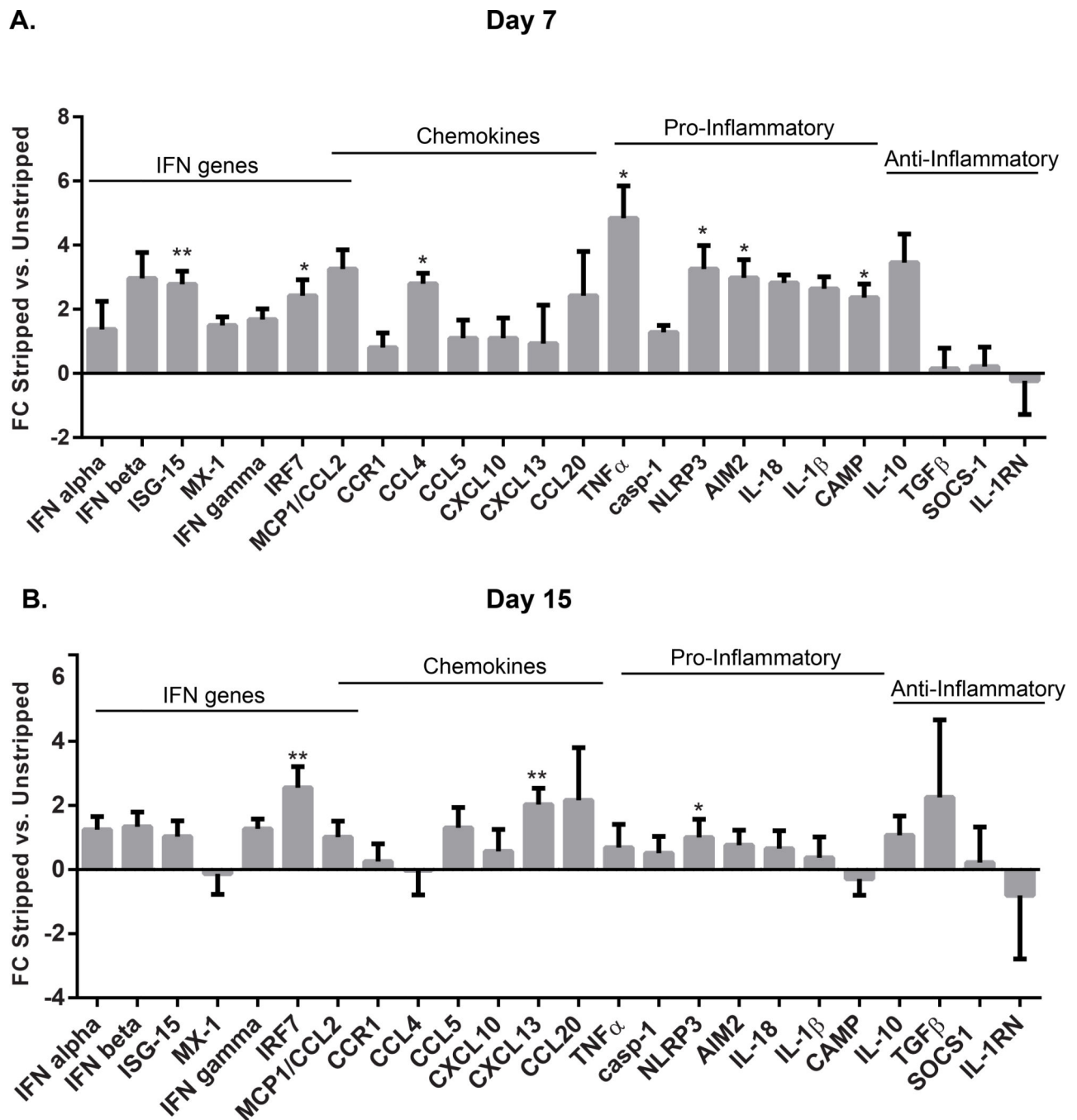


Figure 6. Tape stripping results in induction of inflammatory and IFN-responsive genes followed by induction of CXCL13

Kidney RNA was isolated from control (n=3 for day 7 and n=8 for day 15) and skin injured (n=5 for day 7 and n=9 for day 15) mice at 7 (A) and 15 (B) days post injury. Gene expression analysis for the listed genes was completed via real-time PCR. Graphs represent mean+SEM fold change expression for each gene as compared to the average of sham-injured littermate controls. Significance was calculated using Student's t-test with Welch's

correction for normalized data and Mann-Whitney for non-normalized data via comparison of delta-CTs for sham vs. skin injured mice. *=p<0.05, **=p<0.01.

Author Manuscript

Author Manuscript

Author Manuscript

Author Manuscript

Table 1

Summary of treatments and findings in injured mice.

Day	Treatment	Findings
0	Serum and urine collected	
1	Tape Strip or Sham treatment	Skin: Increased neutrophilic epidermal inflammation
7	Euthanize for day 7 time point	Skin: epidermal hyperplasia and chronic inflammatory changes Kidney: Increased macrophage infiltration; rise in renal inflammatory gene expression
14	Serum and urine collected, Tape Strip or Sham treatment	
15	Euthanize for day 15 time point	Kidney: increased immune complex deposition, increased DC and macrophage infiltration; resolution of inflammatory gene expression but increase in CXCL13.
30, 60	Serum and urine collection, organ harvest at euthanasia (at the onset of proteinuria)	Skin: in surviving mice, rash is persistent and demonstrates lymphocytic and mast cell dermal inflammation. Serum: Drop in dsDNA titers, C3 and serum DNA correlates with rapid development of proteinuria and death. Kidney: Profound renal inflammation at proteinuria onset